Supplementary Information

Improved photophysical properties and durability of $CsPbBr_3$ NCs endowed by inorganic oxoacid and bromide ions

Shuhua Chen,[‡,a] Qixuan Zhong,[‡,a] Jun Liu,[a] Wenhao Guan,[a] Pengli Li,[a] Israr Mahmood,[a] Muhan Cao[,a] and Qiao Zhang[a]*

[a] Institute of Functional Nano and Soft Materials (FUNSOM), Jiangsu Key Laboratory for Carbon-Based Functional Materials and Devices, Soochow University, 199 Ren'ai Road, Suzhou, 215123, Jiangsu, People's Republic of China

E-mail: mhcao@suda.edu.cn (M.C.)

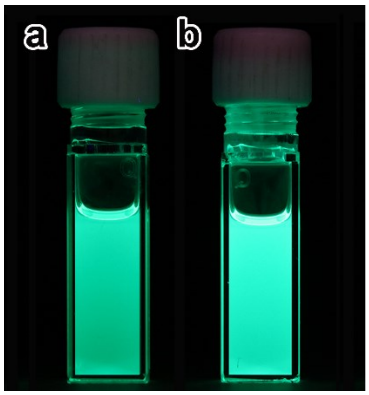

Fig. S1. Photographs of (a) $CsPbBr_3$ and (b) $CsPbBr_3$-P-Br NC solution under 365 nm UV light.

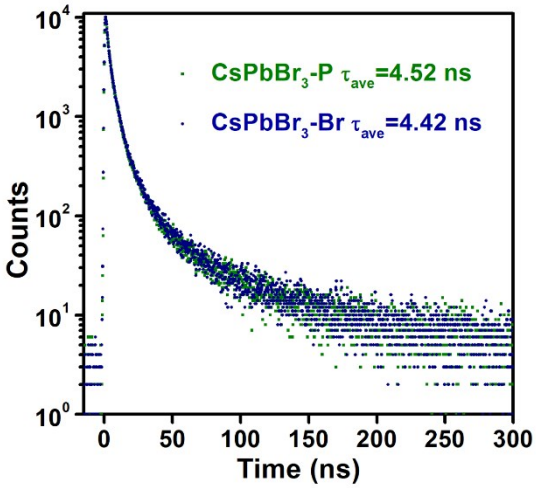

Fig. S2. Time-resolved PL decay curves of $CsPbBr_3$-P NCs and $CsPbBr_3$-Br NCs.

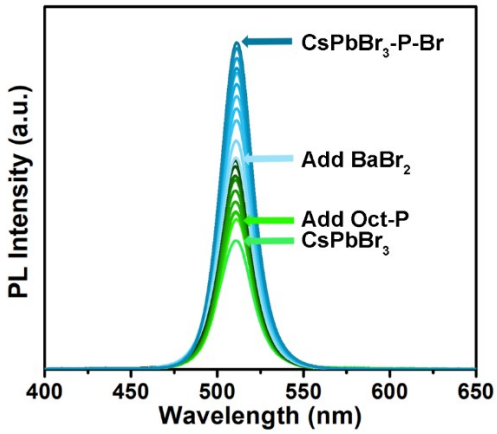

Fig. S3. *In-situ* PL intensity during the rection process. Oct-P was added and kept for 20 min in the first step, followed by adding $BaBr_2$ solution and reacted for another 20 min. Time interval is 2 min.

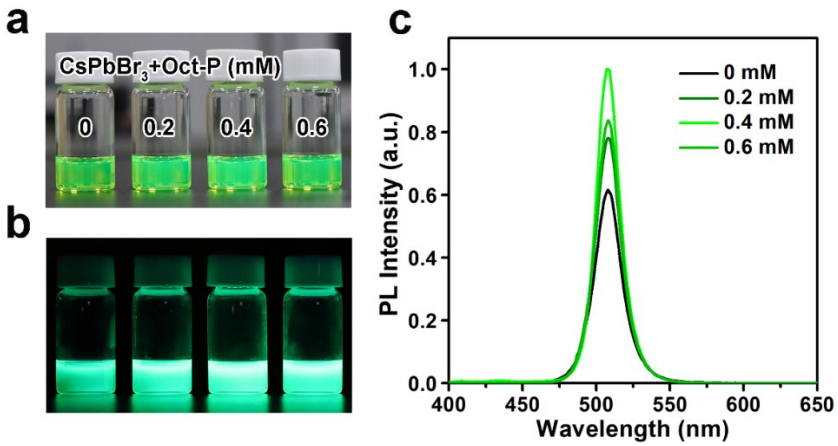

Fig. S4. Photographs of $CsPbBr_3$ NCs treated by Oct-P with different concentrations under (a) daylight and (b) 365 nm UV light. (c) PL intensity of $CsPbBr_3$ NCs treated by Oct-P with different concentrations.

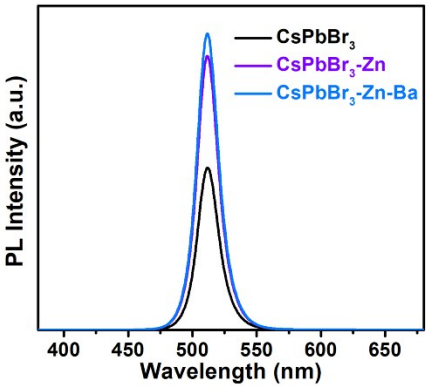

Fig. S5. PL spectra of pristine $CsPbBr_3$ NCs, $CsPbBr_3$-Zn NCs and $CsPbBr_3$-Zn-Ba NCs.

To further confirm the role of Ba^{2+}, we carried out a controlled experiment, in which $CsPbBr_3$-P NCs were passivated by $ZnBr_2$ (1 mM) followed by $Ba(C_2H_3O_2)_2$ (1 mM). PL spectra in Fig. S5 show that the PL intensity of $CsPbBr_3$ NCs increases from 70% to 92% upon the addition of $ZnBr_2$, and further enhanced to 95% in the presence of $Ba(C_2H_3O_2)_2$, very closed to that of $BaBr_2$ (97%). It can be concluded Ba^{2+} can acts as a passivator for $CsPbBr_3$ but no significant improvement can be found when compared with Zn, Pb and Na, probably due to its trace amount.

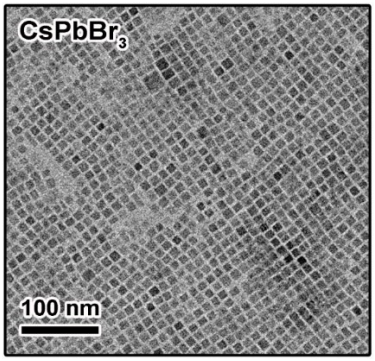

Fig. S6. TEM image of pristine $CsPbBr_3$ NCs.

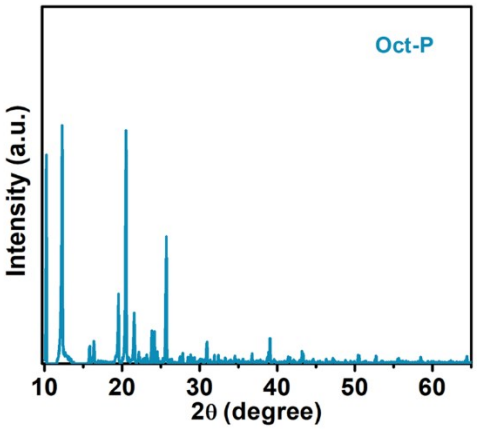

Fig. S7. XRD pattern of the prepared Oct-P powder.

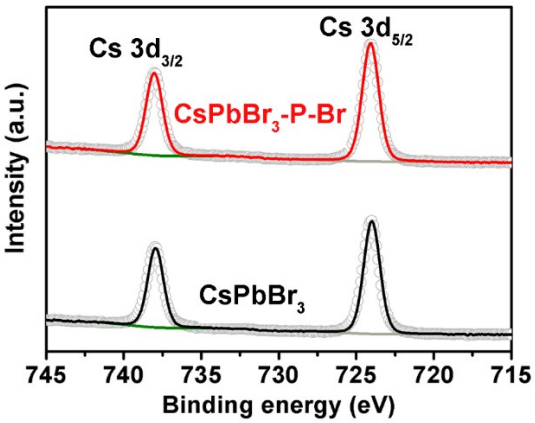

Fig. S8. XPS spectra of Cs 3d from $CsPbBr_3$-P-Br NCs and $CsPbBr_3$ NCs.

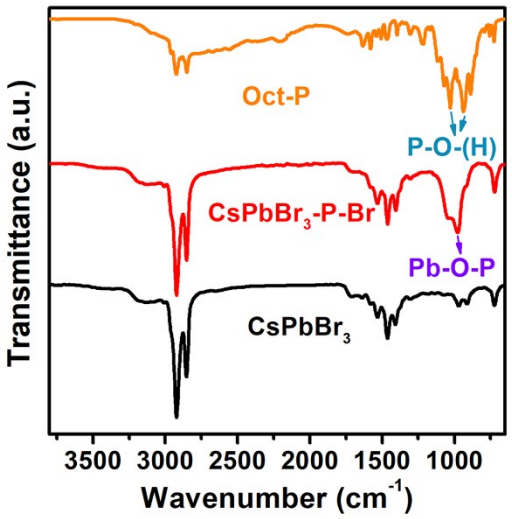

Fig. S9. Fourier transform infrared spectroscopy (FTIR) spectra of Oct-P, pristine $CsPbBr_3$ and $CsPbBr_3$-P-Br NCs.

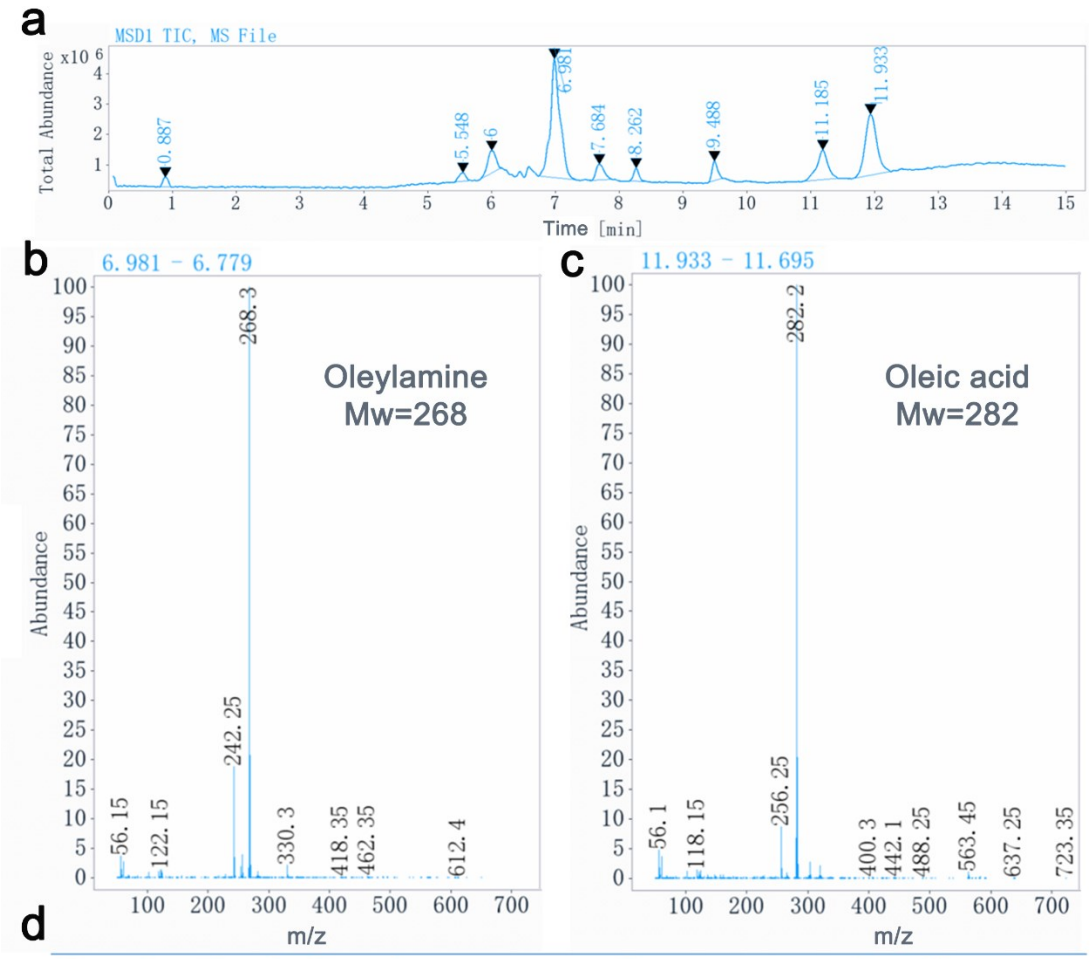

Retention Time (min)	m/z	Component	Area%
6.981-6.779	268	Oleylamine	40.5518
11.933-11.695	282	Oleic acid	25.3423

Fig. S10. (a) Chromatogram from HPLC analyses of pristine $CsPbBr_3$ NCs. MS spectra at retention times of (b) 6.981-6.779 min, (c) 11.933-11.695 min and (d) a table showing the ratio.

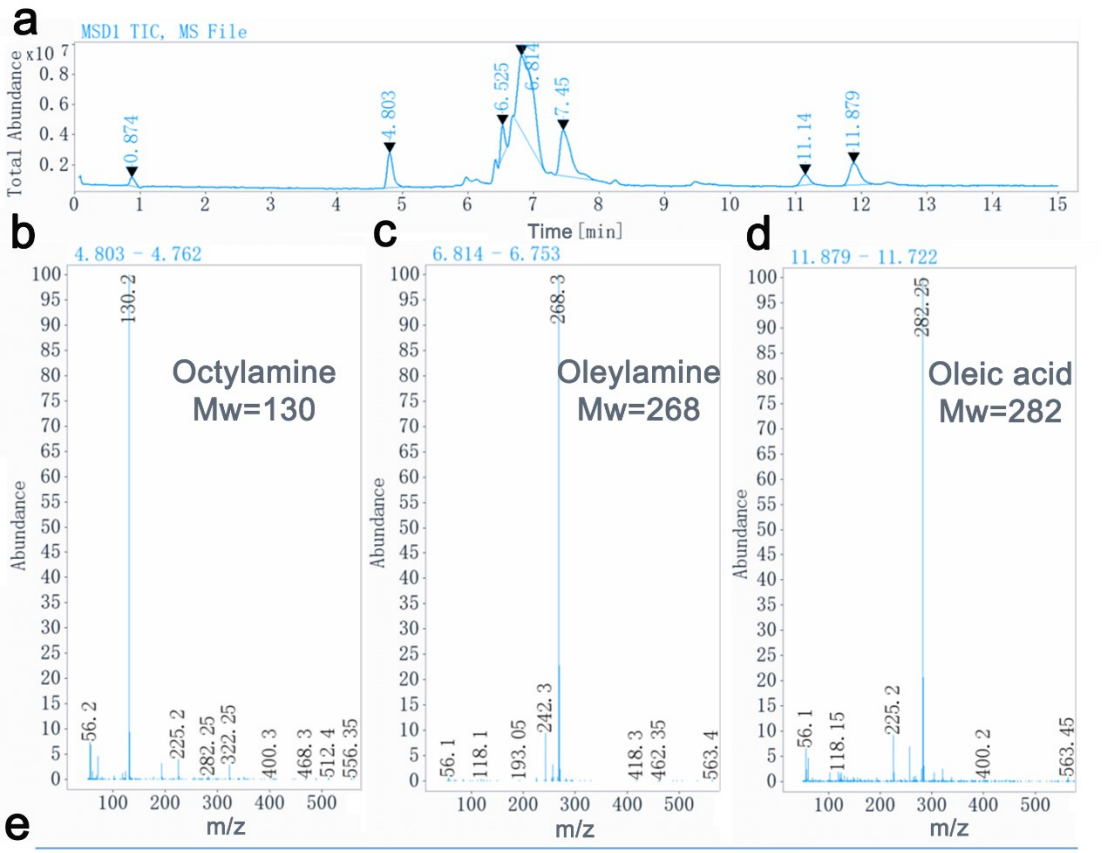

e

Retention Time (min)	m/z	Component	Area%
4.803-4.762	130	Octylamine	8.5704
6.814-6.753	268	Oleylamine	48.8443
11.879-11.722	282	Oleic acid	9.9114

Fig. S11. (a) Chromatogram from HPLC analyses of $CsPbBr_3$-P NCs purified by centrifugation. MS spectra at retention times of (b) 4.803-4.762 min, (c) 6.814-6.753 min, (d) 11.879-11.722 min and (e) a table showing the ratio.

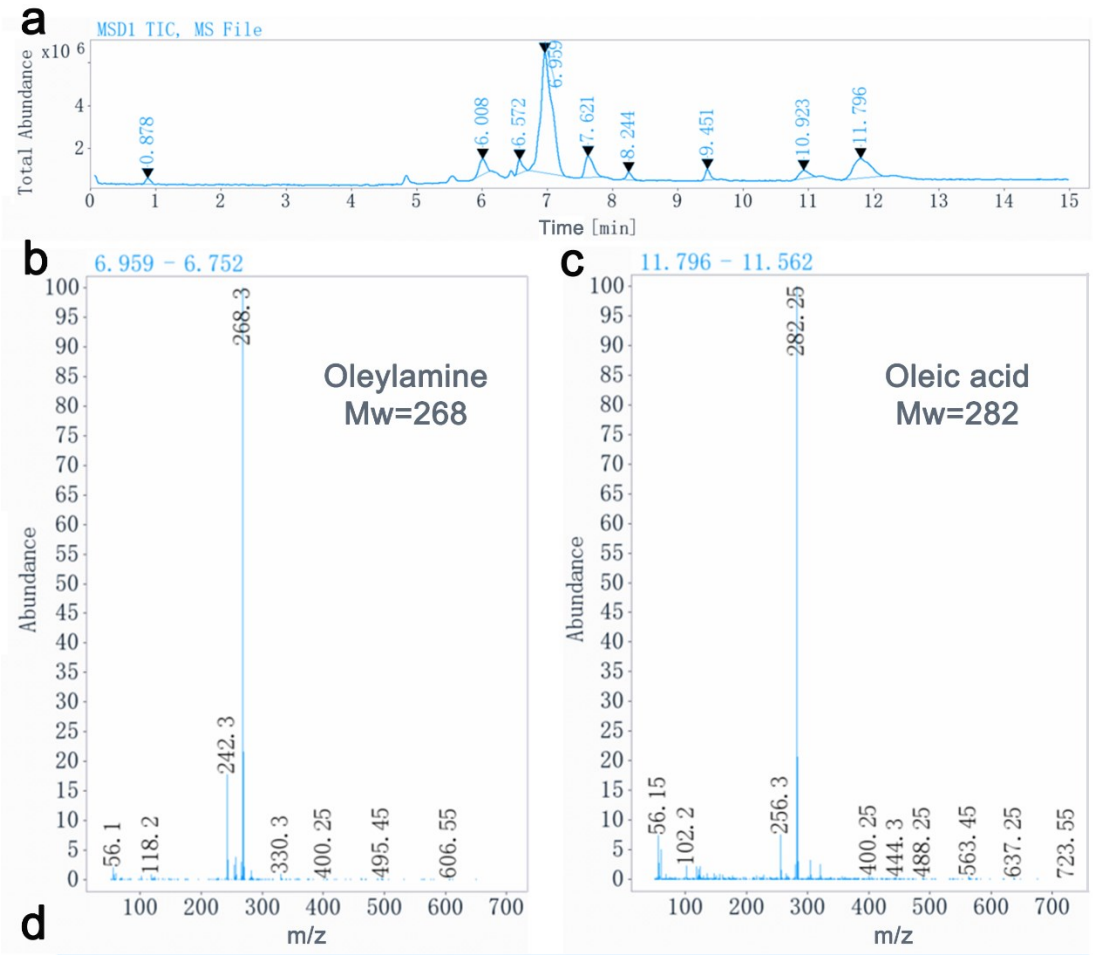

d

Retention Time (min)	m/z	Component	Area%
6.959-6.752	268	Oleylamine	59.9901
11.796-11.562	282	Oleic acid	12.4687

Fig. S12. (a) Chromatogram from HPLC analyses of $CsPbBr_3$-P NCs purified by ethyl acetate. MS spectra at retention times of (b) 6.959-6.752 min, (c) 11.796-11.562 min and (d) a table showing the ratio.

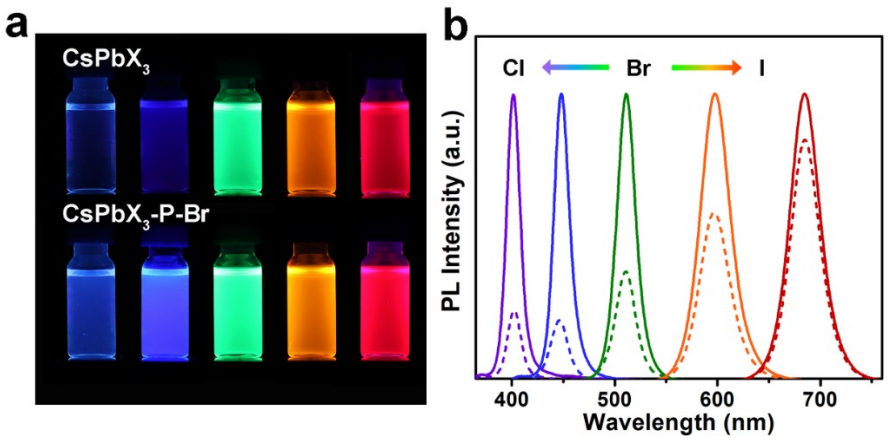

Fig. S13. (a) Photographs of $CsPbX_3$ NCs and $CsPbX_3$-P-Br NCs under 365 nm UV light (X=Cl, $Cl_{0.5}Br_{0.5}$, Br, $Br_{0.5}I_{0.5}$, I, from left to right); (b) Corresponding PL intensity of $CsPbX_3$ NCs and $CsPbX_3$-P-Br NCs, dashed lines are pristine $CsPbX_3$, and solid lines are $CsPbX_3$-P-Br.

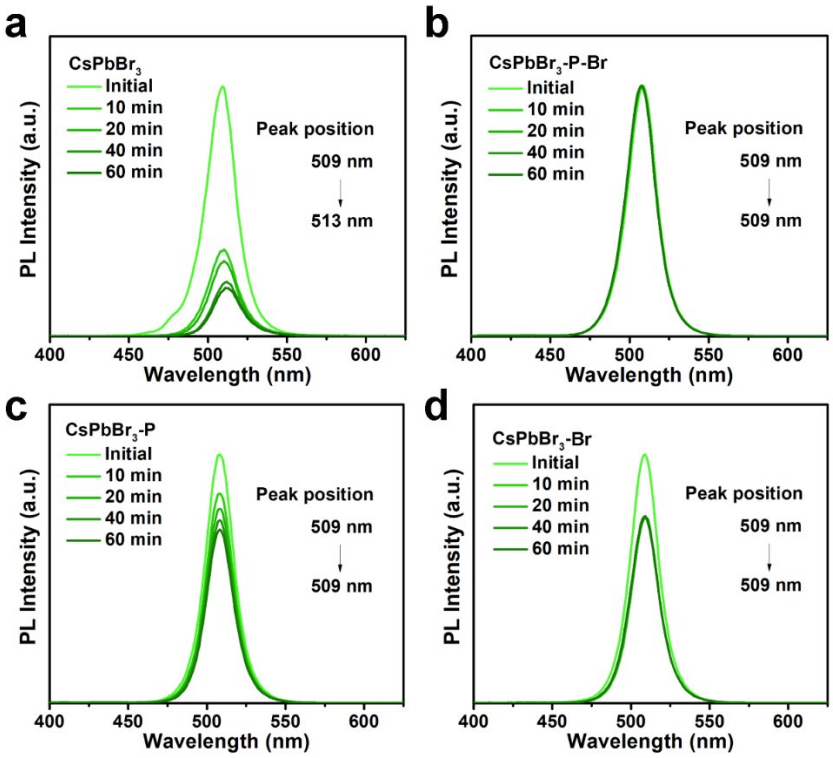

Fig. S14. Time-dependent PL spectra of (a) $CsPbBr_3$, (b) $CsPbBr_3$-P-Br, (c) $CsPbBr_3$-P, and (d) $CsPbBr_3$-Br in the presence of acetone.

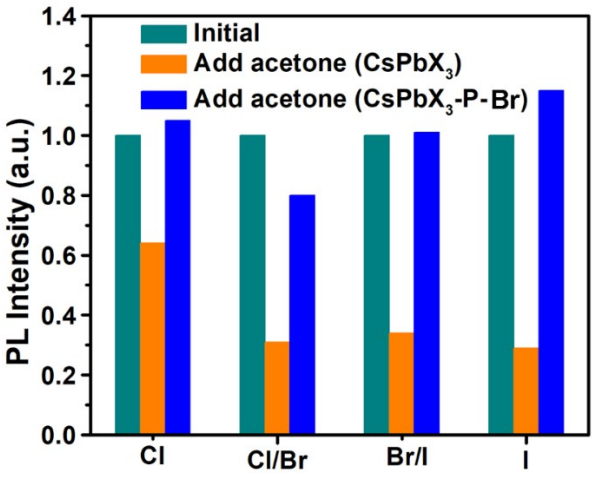

Fig. S15. PL intensity change of $CsPbX_3$ NCs and $CsPbX_3$-P-Br NCs (X=Cl, $Cl_{0.5}Br_{0.5}$, $Br_{0.5}I_{0.5}$, I) after adding acetone for 60 min.

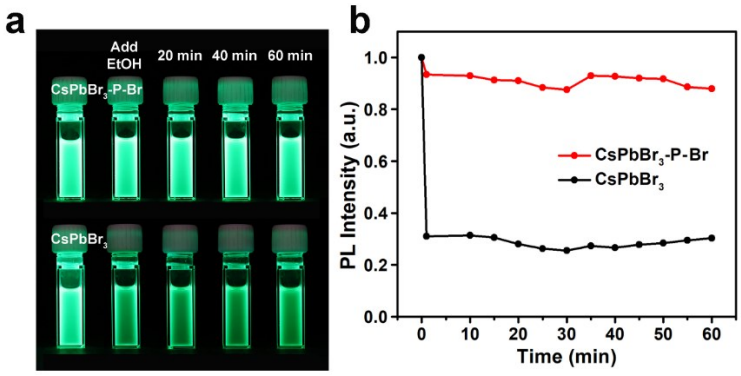

Fig. S16. (a) Photographs of $CsPbBr_3$-P-Br and $CsPbBr_3$ NCs after adding 100 μL ethanol under 365 nm UV light, (b) corresponding PL intensity change.

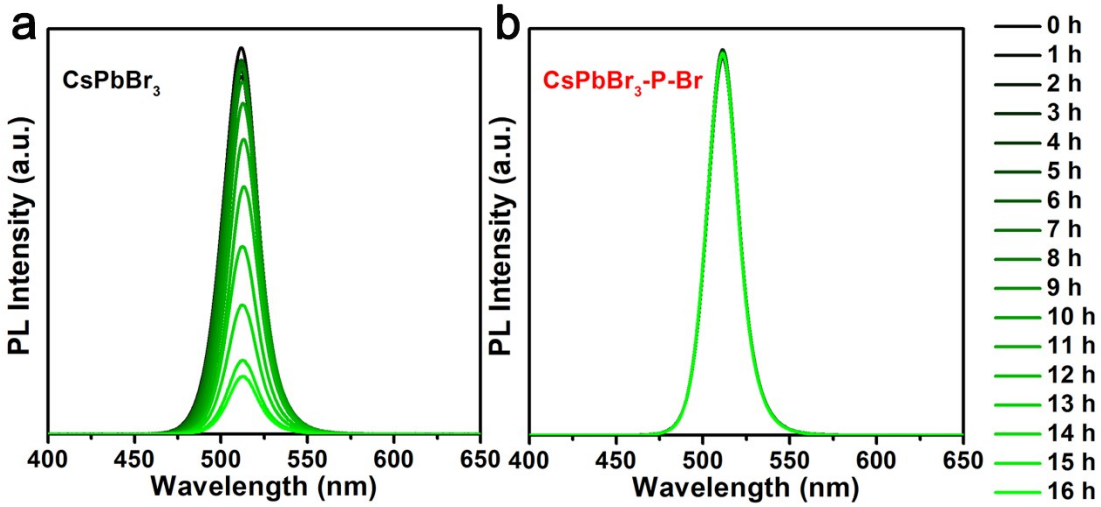

Fig. S17. Time-dependent PL spectra of (a) $CsPbBr_3$ NCs and (b) $CsPbBr_3$-P-Br NCs under 365 nm UV light illumination.

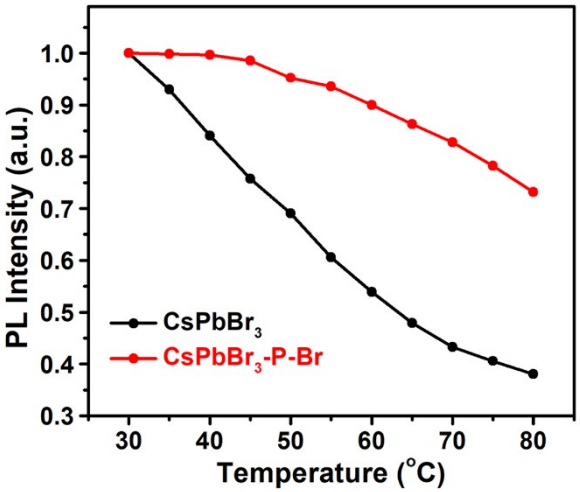

Fig. S18. Temperature-dependent PL intensity of $CsPbBr_3$ NCs and $CsPbBr_3$-P-Br NCs.

Table S1. Detailed information of PL decay.

	τ_1 (ns)	A_1 (%)	τ_2 (ns)	A_2 (%)	τ_3 (ns)	A_3 (%)	τ_{ave} (ns)
$CsPbBr_3$	7.66	21	51.8	1	2.34	78	3.95
$CsPbBr_3$-P	7.75	26	42.9	2	2.3	72	4.52
$CsPbBr_3$-Br	7.13	32	37.1	2	2.12	66	4.42
$CsPbBr_3$-P-Br	4.29	97	16.6	3	-	-	4.66

From the results, $CsPbBr_3$-P and $CsPbBr_3$-Br NCs have a PL lifetime of 4.52 ns and 4.42 ns, respectively, which are longer than that of pristine $CsPbBr_3$ but shorter than that of $CsPbBr_3$-P-Br. From their detailed components, it can be found that the photon-radiative recombination τ_1 increases from 21% to 26% ($CsPbBr_3$-P), 32% ($CsPbBr_3$-Br) and finally to 97% ($CsPbBr_3$-P-Br). The longer-lived component τ_2 may be ascribed to the shallow trap-mediated radiative recombination, which has no significant change upon the treatment. τ_3, the indirect-radiative recombination, decreases to 72% ($CsPbBr_3$-P), 66% ($CsPbBr_3$-Br), and vanishes upon the two-step treatment, suggesting that the trap states are removed from the NCs. From the values, it seems that Br^- ions can better passivate $CsPbBr_3$ NCs. However, PO_4^{3-} is found to play a significant role in tuning the long-chain capping ligand composition (Fig. S10-S12), which is found to be a key step for the subsequent Br^- treatment.

Table S2. Atomic fraction of Cs, Pb, Br, P, Ba determined from EDX element mapping.

Elements	Cs	Pb	Br	P	Ba
Atomic Fraction (%)	18.71	19.52	56.48	4.89	0.4

Table S3. Zeta potential values of different samples in toluene.

	Positive voltage (mV)	Negative voltage (mV)	Average voltage (mV)
$CsPbBr_3$	10.82	11.91	11.36
$CsPbBr_3$-P	52.81	43.93	48.37
$CsPbBr_3$-Br	-9.07	-10.4	-9.73
$CsPbBr_3$-P-Br	25.94	25.10	25.52

*Due to the low conductivity of nonpolar solvent toluene, we selected positive voltage and negative voltage for zeta potential measurement. All the samples were washed by ethyl acetate prior to the test.